GEOPHYSICAL RESEARCH LETTERS, VOL. 28, NO. 24, PAGES 4659-4662, DECEMBER 15, 2001

Forward mechanical modeling of the Amenthes Rupes thrust fault on Mars

Richard A. Schultz[1] and Thomas R. Watters[2]

Abstract. Amenthes Rupes overlies one of the largest thrust faults on Mars, with structural topography accurately measured by MOLA. Forward mechanical models successfully predict the surface topography across this large contractional structure. The best-fitting fault parameters are: fault dip angle, 25–30°; depth of faulting, 25–30 km; and fault offset, 1.5 km. These first-order results are insensitive to either the offset distribution along the fault or crustal material properties. Both very shallow (e.g., ~15 km) and very deep (~45 km) depths of faulting can be ruled out, as can significantly different dips and offset magnitudes. Amenthes Rupes may span the ancient seismogenic lithosphere in the Martian Noachian highlands, implying maximum values at the time of faulting for heat flux of ~54–70 mW m^{-2} and paleogeothermal gradient of 15–20 K km^{-1}.

1. Introduction

For the first time, precision topographic profiling of Martian lobate thrust-fault scarps permits robust mechanical modeling of the structural topography across these large contractional structures. Using topographic measurements acquired by the Mars Orbiter Laser Altimeter (MOLA [*Zuber et al.*, 1992]), the surface topography across lobate scarps on Mars [*Watters*, 1993] can be characterized [*Watters et al.*, 2000]. Here we report results of forward mechanical modeling of MOLA topography from two cross-sectional profiles across Amenthes Rupes. Our results demonstrate: (1) fault dip angles that are consistent with those of strong terrestrial thrust faults having typical frictional strengths [e.g., *Sibson*, 1994], and (2) substantial depths of thrust faulting into the Martian lithosphere.

Amenthes Rupes is recognized as a large surface-breaking Martian thrust fault. The scarp is ~421 km long with maximum structural relief of ~1.3 km [*Watters et al.*, 2000]. The population of lobate scarps that includes Amenthes Rupes formed during the Late Noachian to Early Hesperian [*Watters and Robinson*, 1999] (or ~3.8 Ga in age [*Zuber*, 2001]), deforming ancient highland rocks in an early episode of crustal deformation following the period of heavy bombardment. Because the global-scale effect of Tharsis as recently proposed [*Phillips et al.*, 2001] predicts broad uplift in this region, with slope gradient more nearly parallel to the trends of lobate scarps instead of normal to them, Amenthes and associated lobate scarps may relate more directly instead to the early development of the crustal dichotomy [*Watters*, 1993, 2001; *Watters and Robinson*, 1999]. Our work clarifies the geometry and deformation characteristics of Amenthes Rupes and, in turn, basic properties of the early Martian lithosphere associated with the thrust faulting.

[1] University of Nevada, Reno
[2] National Air and Space Museum, Washington, DC

Paper number 2001GL013468.
0094-8276/01/2001GL013468$05.00

MOLA tracks 10636 and 1639 cross the Amenthes scarp near its center and approximately perpendicular to strike (Figure 1). The structure is a broad asymmetric rise that crests just behind the fault's surface break. The scarp adjoining the surface break slopes upward at ~15°, then back away from the rise crest at ~1°. A subtle trailing depression is present ~60 km behind the surface break (Figure 1). The ~60-km distance between this trailing depression and the surface break defines the cross-strike dimension of the upper plate of the thrust.

2. Methods and Major Parameters

We use the forward mechanical dislocation program Coulomb (available at http://quake.wr.usgs.gov/research/deformation/modeling/coulomb; see *King et al.* [1994], *Toda et al.* [1998], *Schultz* [2000], and *Schultz and Lin* [2001] for applications to faulting) to predict the surface displacements associated with thrust faulting in the Martian crust. The dislocation method [e.g., *Cohen*, 1999] is a standard tool used when the magnitude of offset (relative displacement) along the fault is known, and when the causative remote stress state or frictional/constitutive properties of the fault are unknown [*Rudnicki*, 1980; *Bilham and King*, 1989].

We choose the dislocation approach given that crustal stress states and fault properties during thrust faulting on Mars are

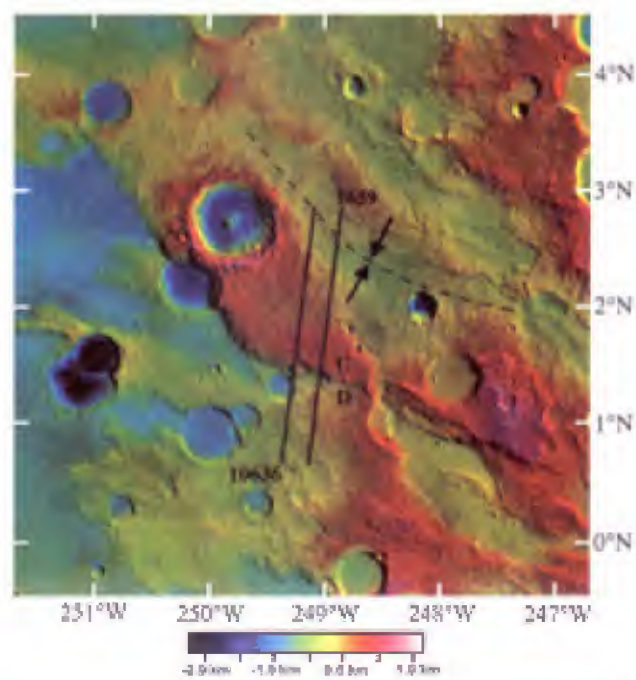

Figure 1. Digital elevation model (DEM; resolution 0.925 km $pixel^{-1}$) from MOLA data showing Amenthes Rupes scarp (thrust plate and hanging wall up, U; lower plate down, D), trailing syncline (curved line with opposing arrows), and positions of MOLA profiles (heavy lines) shown in Figures 2 and 3.

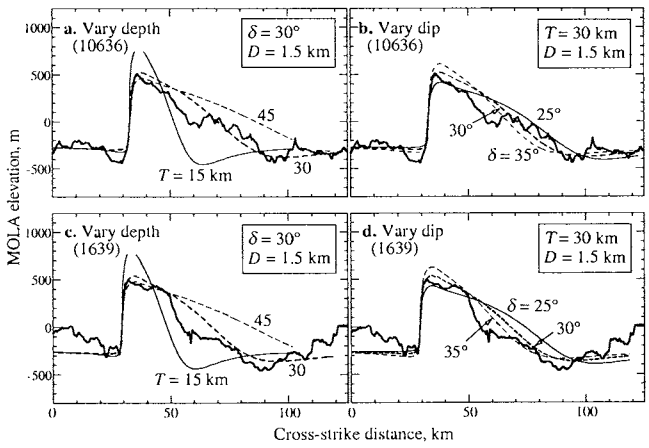

Figure 2. Comparison between calculated surface topography above a surface-breaking thrust fault with MOLA topography for two perpendicular traverses across Amenthes Rupes. Top row (panels a and b), orbit 10636 [*Watters et al.*, 2000]; bottom row (panels c and d), orbit 1639. First column: dip angle δ and offset D held constant, vertical depth of faulting T varied. Second column: depth T and offset D held constant, fault dip δ varied. Vertical exaggeration ~40.6:1 for clarity.

unknown. This approach provides remarkably good fits to the structural topography above a fault for a relatively narrow range of parameters (see discussions by *Cohen* [1999] and *Schultz and Lin* [2001]). Forward mechanical models of faulting can reliably model long-term deformation, and associated near-surface topography, resulting from the cumulative geologic fault offsets, as demonstrated by their application to well-understood terrestrial fault systems [e.g., *King et al.*, 1988; *Bilham and King*, 1989; *Taboada et al.*, 1993; *Crider and Pollard*, 1998].

The magnitude, distribution, and sense of offset are first specified along the fault, then the stresses and material displacements in the vicinity of the fault are completely determined by using the stress functions for an elastic halfspace [*Okada*, 1992]. The halfspace solution increases the near-surface displacements above a thrust fault relative to their values in an infinite faulted medium. An acceptable match (see below) between the model and MOLA topography bounds admissible values. We then calculate the displacement vectors to predict changes in topography due to the surface-breaking thrust fault beneath Amenthes Rupes.

The topography of terrestrial thrust fault scarps is similar to that exhibited across Amenthes Rupes, including maximum structural relief at or behind the surface break and a trailing synclinal depression that marks the approximate vertical location of the lower fault tip in the subsurface [e.g., *Savage and Hastie*, 1966; *King et al.*, 1988; *Taboada et al.*, 1993]. We idealize the fault surface as a rectangular plane having down-dip height H, dip angle δ, and vertical depth of faulting T. We place the lower tip of the Amenthes Rupes thrust fault below the trailing syncline and its upper tip at the surface break; the fault dip angle δ and depth to the lower tip T were then varied to find the parameter ranges that best fit the topography. The magnitude of offset D is estimated initially from the height of the ridge adjacent to the surface break and then adjusted interatively along with δ and T until the best fit with the topography is achieved. The relative-displacement distribution along the thrust fault is taken to be elliptical with a linear taper to within 10 km of the offset minima at the fault tips, comparable to distributions along terrestrial faults [e.g., *Rudnicki*, 1980; *Bürgmann et al.*, 1994].

We choose a crustal elastic modulus of 80 GPa and Poisson's ratio of 0.25. These values are comparable to those used to model deformation associated with fault offset in the terrestrial continental crust [e.g., *Freed and Lin*, 1998]. Reducing the modulus to 40 GPa, and changing Poisson's ratio to either ~0 or 0.5, lead to negligibly small changes in the predicted topography.

We explored the characteristics of predicted structural topographies by systematically varying maximum offsets D from 1.0 to 2.9 km, fault dip angles δ from 15° to 45°, and depths of faulting T (lower fault tip) of 15 to 40 km with offset distributions (linear, elliptical, various tapered elliptical ones, and constant) and the crustal rock properties noted above; for brevity we illustrate only a subset of our parameter variations (Figure 2). Excellent fits to the MOLA topography are obtained by iteratively adjusting the values in the mechanical model. Although some variation in the parameters is permitted by the data, a remarkably good match is obtained for a relatively narrow range of the fault parameters. The fits were verified by quantitatively comparing the predicted and observed topographies for each class of runs (not shown).

3. Results

The best fits to the MOLA topography across Amenthes Rupes are obtained by using depth of faulting T = 25–30 km, fault dip angle δ = 25–30°, and D = 1.5 km of offset along the fault with a tapered elliptical distribution (Figure 3). On the basis of the mechanical analysis, several extreme values can be ruled out. Specifically, we find that depths of faulting $T \ll 30$ km (see Figure 2, curves for 15 km) and $T \gg 30$ km (Figure 2, 45-km curves) produce unacceptable fits to the MOLA data. The shallower depths of faulting ($T < 25$ km) move the trailing syncline beneath the elevated portion of the upper plate, whereas deeper T's would produce excessive topography and upper plate width. Reducing the fault dip angle to 25° leads to effects similar to, though not as pronounced as, deeper T, whereas increasing the dip to 35° steepens the predicted ridge topography somewhat but overestimates the magnitude of displacement at the surface scarp.

Changing the fault geometry to a listric shape (modeled but not shown) leads to unacceptably poor fits to the topography. As fault dip shallows with depth, the offsets along the lower parts of the fault interact more readily with the surface, leading to greater (vertical) structural relief behind the surface break. However, the trailing syncline is enlarged significantly in width and depth by offset along either a shallowly dipping thrust fault or one that merges into a basal décollement. At most, the Amenthes fault may shallow from ~30° to ~25° as it approaches depths of 25–30 km. The modeling suggests that the thrust fault does not sole into a subhorizontal décollement at depth.

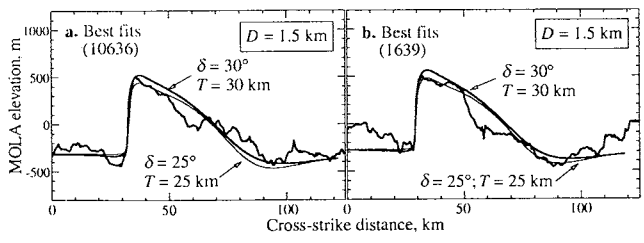

Figure 3. Best-fitting thrust-fault models for Amenthes Rupes. Both plots compare the same sets of curves to orbital tracks 10636 (a) and 1639 (b) and assume 1.5 km offset along the fault.

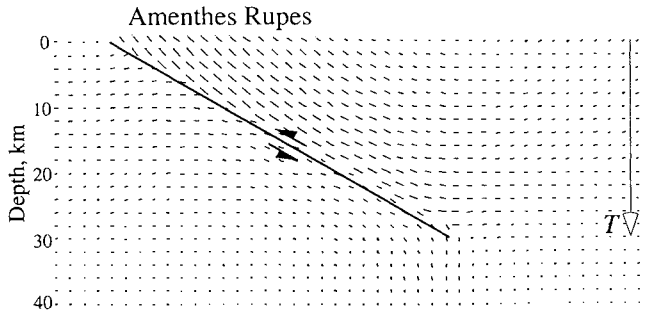

Figure 4. Trajectories of material displacements in the Martian crust calculated from best-fitting case for Amenthes Rupes (D = 1.5 km, δ = 30°, T = 30 km). Displacements of crustal rocks (tick marks, lengths proportional to local displacement magnitude) shown as 5x actual magnitudes; no vertical exaggeration.

Increasing the offset magnitude along the thrust fault to 1.6 km increases the amplitude of predicted topography, leading to a poorer fit to the profiles than the 1.5 km used. The distribution of relative displacement (offset) along the fault (constant [not shown] vs. elliptical vs. linearly vary-ing) also influences the fits somewhat. The tapered elliptical distribution (Figures 2 and 3) slightly over-predicts the near-scarp topography for smaller T but generally improves the fit overall compared to the other distributions, especially at the location of the surface break. Further justification for this offset distribution is based on examining the topography where the fault breaks the surface. The Amenthes Rupes thrust fault cuts across the floor of a ~30 km diameter impact crater (Figure 1). The trace of the fault is associated with a vertical uplift of the crater floor material of < 100 m (MOLA track 10460). This suggests that the cumulative structural relief on Amenthes Rupes (~1.5 km) mainly developed while the thrust fault was blind and propagating up toward the surface [e.g., *Niño et al.*, 1998].

Both MOLA profiles contain topographic variations on the upper plate not accounted for by a single underlying thrust fault. Examination of the DEM (Figure 1), Viking images, and MOLA profiles suggests that a rectilinear depression crosscuts the upper plate ~10 km behind the surface break (see Figure 2), perhaps contiguous with the scarp-parallel fault that crops out to the south. This depression has the effect of locally decreasing part of the relief in the structural uplift above the fault plane. Similarly, crater ejecta locally adds excess relief to the upper plate. However, the trailing syncline marks the topographic inflection in both MOLA profiles and the approximate end of the upper plate of the thrust wedge.

The relief of Amenthes Rupes where MOLA tracks 10636 and 1639 cross the structure is approximately 800 m (Figure 1, 2). The maximum relief h of Amenthes Rupes, based on MOLA track 15000, is about 1.27 km and occurs roughly 40 km to the northwest of MOLA track 10636 (see Figure 1). Previous estimates of offset on Martian thrust faults (including Amenthes Rupes) have been made from kinematic reconstruction of scarp offsets using measured scarp relief h and assumed values for fault dip δ [*Watters et al.*, 2000, their Fig. 2]. The kinematic offset is given trigonometrically by $D = h/\sin\delta$, and for h = 800 m and δ = 30°, D = 1.6 km. These results are consistent with the values of offset (1.5 km) and fault dip angle (25–30°) obtained independently in our mechanical model for the section of the Amenthes Rupes thrust fault being investigated.

4. Implications

We infer that Amenthes Rupes deforms a substantial volume of the Martian crust down to ~25–30 km (Figure 4). The depth of faulting is comparable to independent estimates of the effective elastic thickness T_e of the highlands of Terra Cimmeria and along the dichotomy boundary ($T_e \cong$ 20–30 km) [*Zuber et al.*, 2000; *Nimmo*, 2001]. The effective elastic thickness (in the absence of bending or localized deformation) is thought to correlate approximately with the depth of the 450°–600°C isotherm below which a planetary interior is too weak to support long-term (elastic) stresses [e.g., *Watts et al.*, 1980; *Tse and Rice*, 1986; *McKenzie and Fairhead*, 1997]. On Earth's continents, T_e is comparable to the thickness of the seismogenic crust T_s [*McKenzie and Fairhead*, 1997; *Maggi et al.*, 2000]. If the Amenthes Rupes thrust fault attains a depth of ~30 km and if the terrestrial results are applicable to Mars, then the fault may transect the entire elastic and seismogenic lithosphere in the Martian highlands. Assuming plausible if approximate values of $T_e \cong$ 30 km, a temperature 725–875 K at the base of the elastic lithosphere, a surface temperature of 220 K [*Nimmo and Stevenson*, 2001], a thermal conductivity of 3.2 W m^{-1} K^{-1}, and a linear temperature variation in the lithosphere [*Nimmo and Stevenson*, 2001], we estimate a maximum heat flux of perhaps ~54–70 mW m^{-2} and maximum paleogeothermal gradient of 15–20 K km^{-1} at the time Amenthes Rupes formed. These ranges are consistent with those obtained for Terra Cimmeria from a lithospheric thickness inversion (15–22 K km^{-1} and 38–57 mW m^{-2}) [*Zuber et al.*, 2000], and are about twice suggested values for the present-day heat flux [*Nimmo and Stevenson*, 2001].

The fault dip angle, 25–30°, is consistent with those of terrestrial thrust faults located outside of fold-and-thrust belts and with values of friction (μ = 0.6) typical of terrestrial crustal rocks [e.g., *Sibson*, 1994; *Beeler et al.*, 2000]. Our work confirms the applicability of 'Byerlee' friction parameters and friction laws to Martian faults while implying that they are frictionally strong. It also demonstrates how the wide range of possible fault dips, as noted in the literature for Martian faults [e.g., *Watters*, 1993; *Schultz and Lin*, 2001], can be narrowed considerably by mechanical modeling of MOLA topography.

The deformation associated with thrust faulting is spatially inhomogeneous, varying significantly in magnitude with location, from the surface break back to the trailing syncline. The strain at the Martian surface—within the upper plate—decreases from a maximum near the position of the surface break toward zero in the trailing syncline (see Figure 4). Such spatial variations are not incorporated in simple rigid-block kinematic models of planetary faulting. We conclude that forward mechanical models of thrust fault deformation provide a powerful tool for interpreting MOLA topography across faulted Martian terranes and thereby reconstructing the regional tectonics.

Acknowledgments. This work was supported in part by grants from NASA's Planetary Geology and Geophysics Program (to R.A.S.) and Mars Data Analysis Program (to T.R.W.). Ross Stein kindly made available the Coulomb boundary element program. Helpful reviews by Francis Nimmo and an anonymous reviewer improved the breadth and clarity of the paper.

References

Beeler, N.M., R.W. Simpson, S.H. Hickman, and D.A. Lockner, Pore fluid pressure, apparent friction, and Coulomb failure, *J. Geophys. Res.*, *105*, 25,533–25,542, 2000.

Bilham, R., and G. King, The morphology of strike-slip faults: Examples from the San Andreas Fault, California, *J. Geophys. Res.*, *94*, 10,204–10,216, 1989.

Bürgmann, R., D.D. Pollard, and S.J. Martel, Slip distributions on faults: Effects of stress gradients, inelastic deformation, heterogeneous host-rock stiffness, and fault interaction, *J. Struct. Geol.*, *16*, 1675–1690, 1994.

Cohen, S.C., Numerical models of crustal deformation in seismic zones, *Adv. Geophys.*, *41*, 133–231, 1999.

Crider, J.G., and D.D. Pollard, Fault linkage: Three-dimensional mechanical interaction between normal faults, *J. Geophys. Res.*, *103*, 24,373–24,391, 1998.

Freed, A.M., and J. Lin, Time-dependent changes in failure stress following thrust earthquakes, *J. Geophys. Res.*, *103*, 24,393–24,409, 1998.

King, G.C.P., R.S. Stein, and J.B. Rundle, The growth of geological structures by repeated earthquakes 1, Conceptual framework, *J. Geophys. Res.*, *93*, 13,307–13,318, 1988.

King, G.C.P., R.S. Stein, and J. Lin, Static stress changes and the triggering of earthquakes, *Bull. Seismol. Soc. Am.*, *84*, 935–953, 1994.

Maggi, A., J.A. Jackson D. McKenzie, and K. Priestley, Earthquake focal depths, effective elastic thickness, and the strength of the continental lithosphere, *Geology*, *28*, 495–498, 2000.

McKenzie, D., and D. Fairhead, Estimates of the effective elastic thickness of the continental lithosphere from Bouguer and free air gravity anomalies, *J. Geophys. Res.*, *102*, 27,523–27,552, 1997.

Nimmo, F., Crustal and elastic thickness estimates at the Martian hemispheric dichotomy (abstract). *Lunar Planet. Sci.*, *XXXII*, abs. #1370 [on CD-ROM], 2001.

Nimmo, F., and D.J. Stevenson, Estimates of Martian crustal thickness from viscous relaxation of topography, *J. Geophys. Res.*, *106*, 5085–5098, 2001.

Niño, F., H. Philip, and J. Chéry, The role of bed-parallel slip in the formation of blind thrust faults, *J. Struct. Geol.*, *20*, 503–516, 1998.

Okada, Y., Internal deformation due to shear and tensile faults in a half-space, *Bull. Seismol. Soc. Am.*, *82*, 1018–1040, 1992.

Phillips, R.J., et al., Ancient geodynamics and global-scale hydrology on Mars, *Science*, *291*, 2587–2591, 2001.

Rudnicki, J.W., Fracture mechanics applied to the Earth's crust, *Annu. Rev. Earth Planet. Sci.*, *8*, 489–525, 1980.

Savage, J.C., and L.M. Hastie, Surface deformation associated with dip-slip faulting, *J. Geophys. Res.*, *71*, 4897–4904, 1966.

Schultz, R.A., Localization of bedding plane slip and backthrust faults above blind thrust faults: Keys to wrinkle ridge structure, *J. Geophys. Res.*, *105*, 12,035–12,052, 2000.

Schultz, R.A., and J. Lin, Three-dimensional normal faulting models of the Valles Marineris, Mars, and geodynamic implications, *J. Geophys. Res.*, *106*, 16,549–16,566, 2001.

Sibson, R.H., An assessment of field evidence for 'Byerlee' friction, *Pure Appl. Geophys.*, *142*, 645–662, 1994.

Taboada, A., J.C. Bousquet, and H. Philip, Coseismic elastic models of folds above blind thrusts in the Betic Cordilleras (Spain) and evaluation of seismic hazard, *Tectonophysics*, *220*, 223–241, 1993.

Toda, S., R.S. Stein, P.A. Reasenberg, J.H. Dieterich, and A. Yoshida, Stress transferred by the 1995 $M_w = 6.9$ Kobe, Japan, shock: Effect on aftershocks and future earthquake probabilities, *J. Geophys. Res.*, *103*, 24,543–24,565, 1998.

Tse, S.T., and J.R. Rice, Crustal earthquake instability in relation to the variation of frictional slip properties, *J. Geophys. Res.*, *91*, 9452–9472, 1986.

Watters, T.R., Compressional tectonism on Mars, *J. Geophys. Res.*, *98*, 17,049–17,060, 1993.

Watters, T.R., Topography of lobate scarps along the dichotomy boundary from MOLA data (abstract), *Lunar Planet. Sci.*, *XXXII*, abs. #1597 [on CD-ROM], 2001.

Watters, T.R., and M.S. Robinson, Lobate scarps and the origin of the Martian crustal dichotomy, *J. Geophys. Res.*, *104*, 18,981–18,990, 1999.

Watters, T.R., R.A. Schultz, and M.S. Robinson, Displacement-length relations of thrust faults associated with lobate scarps on Mercury and Mars: Comparison with terrestrial faults, *Geophys. Res. Lett.*, *27*, 3659–3662, 2000.

Watts, A.B., J.H. Bodine, and N. Ribe, Observations of flexure and the geological evolution of the Pacific Ocean basin, *Nature*, *283*, 532–537, 1980.

Zuber, M.T., The crust and mantle of Mars, *Nature*, *412*, 220–227, 2001.

Zuber, M.T., et al., The Mars Observer Laser Altimeter investigation, *J. Geophys. Res.*, *97*, 7781–7797, 1992.

Zuber, M.T., et al., Internal structure and early thermal evolution of Mars from Mars Global Surveyor topography and gravity, *Science*, *287*, 1788–1793, 2000.

R.A. Schultz, Geomechanics–Rock Fracture Group, Department of Geological Sciences/172, Mackay School of Mines, University of Nevada, Reno, NV 89557–0138 (e-mail: schultz@mines.unr.edu).

T.R. Watters, Center for Earth and Planetary Studies, National Air and Space Museum, Smithsonian Institution, Washington, DC 20560 (e-mail: twatters@nasm1.si.edu).

(Received May 17, 2001; revised August 20, 2001;
accepted September 5, 2001.)